

SYNTHETIC APERTURE SIGNAL PROCESSING FOR HIGH RESOLUTION 3D IMAGE RECONSTRUCTION IN THE THZ-DOMAIN

Marijke Vandewal, Roel Heremans and Marc Acheroy

Royal Military Academy
Renaissancelaan 30, 1000 Brussels, Belgium
phone: + (32) 2742 6563, fax: + (32) 2742 6472,
email: marijke.vandewal@rma.ac.be, roel.heremans@elec.rma.ac.be

ABSTRACT

The purpose of this paper is to demonstrate the application of synthetic aperture imaging used in radar and sonar to the terahertz (THz) domain and to create high resolution three-dimensional images. For this demonstration the paper presents images - based on simulated data - which reveal the performance to be expected of synthetic aperture imaging for different frequencies in the THz band. The processed target responses of pulsed broadband radiation show high resolution which can lead to an improvement of non-destructive defect identification.

1. INTRODUCTION

The terahertz (THz) spectrum covers a frequency spectrum from the far-IR (Infra-Red) region to the mid-IR region (center frequency between 100 GHz and 10 THz [1]). There are three major factors contributing to the interest in this particular frequency band:

- THz radiation is readily transmitted through most non-metallic and non-polarized media, thus enabling THz systems to 'see-through' these materials,
- THz radiation is non-ionizing and poses no health risk to the system's operator,
- the use of high frequencies promises potential for high resolution data when applying imaging techniques.

The NDT (non-destructive testing) community can take advantage of these unique properties of THz radiation, to identify defects such as delaminations, voids and heat damage in a variety of pre-cured and in-service composite structures. For this type of applications high resolution images, preferably in three dimensions, are mandatory. Inefficient generation techniques and high atmospheric absorption constrained early interest and funding for THz gap science. Over the last decade, this THz gap has been bridged over, and with the technological advances, renewed interest [1] has come in high-resolution imaging going beyond the limits imposed by the illuminating beam or the optical sub-elements.

Despite the knowledge that synthetic aperture (SA) processing leads to high resolution images [2], very little research exists in SA using THz radiation. Exceptions are published results related to interferometry rather than actual synthetic aperture imaging [3], [4] or small scale SA results based on THz pulse ranging [5] on reflective and opaque objects. This paper will help to fill up this research gap in two ways:

- the demonstration of the applicability of synthetic aperture processing ([6], [7]) in the THz domain by expanding this imaging technique to the 3rd dimension

- the exploration of the reachable performances by combining THz waves and SA imaging in the domain of NDT.

In this paper we will refer to this approach as SAT which stands for Synthetic Aperture in the THz domain.

In high-resolution 3D imaging two types of spatial resolution need to be defined for pulsed THz systems. The first one is referred to as the depth (or range) resolution which depends on the spectral bandwidth of the pulses and which will not be altered by SA imaging, since it is not diffraction limited. Furthermore this resolution is already almost an order of magnitude smaller than the used peak wavelength because the used pulse width for THz rays (or T-rays) is approximately 100 femtoseconds. The second type of resolution is a 2D azimuth resolution (measured in the plane perpendicular to the pulse direction) which is typically limited by the beam width. Indeed, this azimuth resolution of THz imaging is determined by the Rayleigh criterion (imposed by the used wavelength and the used optics). In classic THz imaging this resolution depends fully on the opening angle of the used THz beam and the distance at which the object is placed from the THz source. Resolution results of classic THz imagers show values that are more or less twice the size of the wavelength for continuous wave (CW) systems (a resolution of 3 mm is obtained with a 0.2 THz CW system [8]). Values of 2 to 3 mm are obtained using a pulsed system [4], [9]-[10]. A set of optics is responsible for keeping the opening angle small and the positioning and fine tuning of these optics need to be done with care [8], [9]. It should be noted that this resolution is only reached for a certain layer within the illuminated object given the so-called beam focusing depth inherent to the used optics. If the requirements on this beam width could be relaxed without deterioration of the azimuth resolution, the hardware would be a lot less complex. This is a first justification for a measurement technique with a wide angle beam, for which the necessary resolution is reached through the application of an appropriate signal processing, in this case the synthetic aperture processing. A second justification lies in the fact that most composite materials have a maximum transparency in the sub-THz domain (typically between 0.1 and 0.8 THz). The use of a laser source to create T-rays in a very broad band is therefore not necessary because the advantage of using a very short wavelength (to reduce the beam width) by going very high in the THz frequency band cannot be used. Using a THz wave generator and an antenna to propagate the waves would only make use of the sub-THz but would also imply beams with a wide opening angle. At this point the synthetic aperture processing comes again in play since it will use this wide opening angle as an

advantage. The benefits of SA processing applied to THz waves versus the classic THz imaging can be summarized as follows:

- SA processing promises to achieve a better resolution than the ones from the traditional THz imaging systems with less constraints on the needed optics,
- this resolution will be constant for every considered depth and thus will not depend on a certain focusing depth linked to the used optics.

The following methodology has been applied in this paper: at first the 3D imaging concept based on the SA principle is explained using simulated data from a sensor moving along multiple tracks in a given plane. These recorded data are called the raw (unprocessed) data. The structure of the SAT raw data simulator is explained for point target defects in a transparent medium. This simulator allows verification and validation of the developed SA processing algorithm presented next. The performances (in terms of resolution) of the 3D imaging technique will be evaluated for different THz frequencies. The paper concludes with the analyzed results and achievements, and the future research work.

2. RAW DATA GENERATION

2.1 Concept of 3D synthetic aperture

The principle of classical SA imaging [2] is the reconstruction (pixel by pixel) of the image by coherently summing along a 2D range migration hyperbole obtained by the 1D (along-track) scanning of the scene using a wide beam. Indeed, in the concept of Synthetic Aperture Radar (SAR) and Sonar (SAS) processing, the so-called azimuth compression reduces the echo return from a point scatterer characterized by a hyperbole into a single point. Conventional SAR or SAS processing, however, uses only one track following the along-track displacement of the sensor, in SAT multiple parallel along-tracks (see Fig.1) are taken into consideration. Such a 2D scanning leads to a hyperboloid echo response for a point target whereas if the scanning were performed along a single track the point target response would have been a cross section of the hyperboloid, being a hyperbole. The aim of SAT processing is to compress this hyperboloid in both the u - and v -direction [11] (see Fig. 2) into a single point response where the third coordinate contains depth information. Adding this extra scanning dimension reveals in the image reconstruction three dimensional position information. This 3D (u, v, z) reconstruction will be explained in section 3.

2.2 Generation of raw data set

Based on the measurement configuration illustrated in Fig. 1 one can see that the response of a transmitted THz pulse¹ can be simulated for each sensor position (u_s, v_s, z_s) , with a delay time characterized by the distance from the sensor to the target position (u_t, v_t, z_t) . The distance for a chosen $z_s = 0$ is given by

$$d_t = \sqrt{(u_s - u_t)^2 + (v_s - v_t)^2 + z_t^2} \quad (1)$$

The simulator takes a rectangular footprint into account characterized by δ_u and δ_v (mm) in respectively the u - and v -

¹Here a rectangular pulse is considered as the input pulse with a length of τ seconds (see Table 1) and a single carrier frequency f_0 .

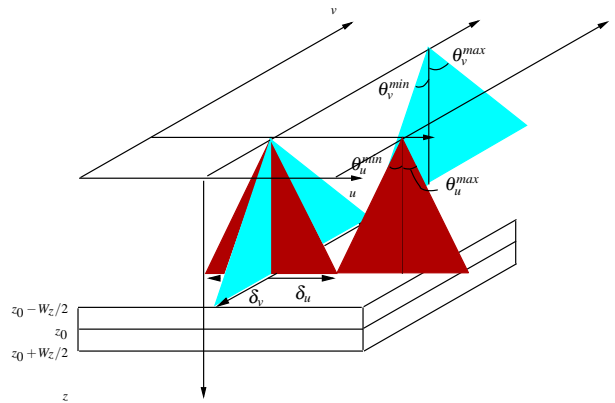


Figure 1: Geometry of the THz scanning- and target field.

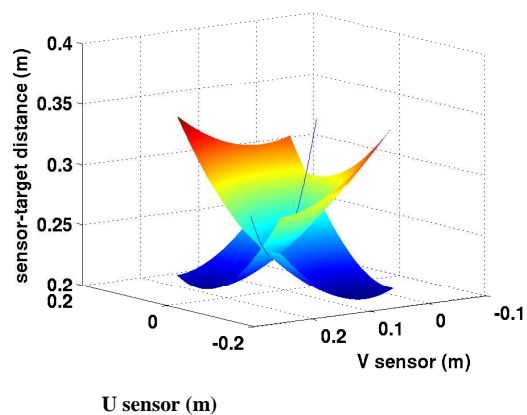


Figure 2: 3D representation of the delay-time as a function of the sensor-position for 2 targets placed at $(u_t, v_t, z_t) = (-0.113, 0.05, 0.2)$ and $(0.068, 0.2, 0.202)$ where the three coordinates are expressed in meters. The line represents the spatial coordinates where the two hyperbolas intersect.

direction. The footprint is determined by the opening angles θ_u and θ_v and the depth z under consideration following, $\delta_{u,v} = 2z \tan(\theta_{u,v}/2)$. The system parameters that were used in the simulator are summarized in Table 1. The working principle of the raw data simulator has been explained in details in [11]. For every position of the sensor on the respective tracks, the response of the defined point targets is calculated and stored on the corresponding position in a 3D matrix. The amplitude and phase of a target response depend on the position of the target with respect to the sensor and more in particular the range between them. The output of the simulator is the 3D raw data matrix containing in each cell the added amplitude and phase information of the respective point targets.

3. 3D SYNTHETIC APERTURE PROCESSING

Whereas in [3] the term synthetic aperture is used to reconstruct the image through Fourier inversion of detector pair correlations, here the terminology refers to the conventional synthetic aperture used to reconstruct the high resolution im-

$f_0 = 0.16 / 0.3 / 1 \text{ THz}$	
$\theta = 20^\circ / 30^\circ$	
$V = 1 \text{ m/s}$	$PRF = 2100 \text{ Hz}$
$z_0 = 0.2 \text{ m}$	$W_z = 0.2 \text{ m}$
$\tau = 1.8 \text{ ps}$	$c = 299792458 \text{ m/s}$

Table 1: THz parameters used in the target response simulation.

age [12]. The position of the sensor at transmission time (u_s, v_s) is assumed to be known within wavelength accuracy. To reconstruct the synthetic aperture THz image, a time domain reconstruction algorithm is used. This 3D algorithm is an extrapolation of the 2D version well known in SAR and SAS. The algorithm is rather slow but very accurate. In this phase of the research the precision of the processing algorithm is an appreciated advantage in the validation of the performance of 3D SA imaging in the THz domain. The *time domain algorithm* [2] can be easily understood based on the configuration of the raw data matrix: for each grid point in the final 3D image the interpolating value on the raw data matrix is summed coherently (since the phase information is crucial in SA processing) corresponding to the back-projected range distance d , defined as

$$d_r = \sqrt{(u_r - u_s)^2 + (v_r - v_s)^2 + z_r^2} \quad (2)$$

where the index r refers to the reconstruction grid. The back-projected range distance is the same as in equation (1) except from the fact that the target location has been replaced by the reconstructed image pixel location. The number of coherently summed echoes for each reconstructed image pixel depends on the beam widths θ_u and θ_v and the shape of the hyperboloid, and is referred to as a 2D range migration. The latter is different for every considered depth; the processing algorithm needs to take this dependency carefully into account. The coherent sum consists of a double sum, one over the echoes in the measured u -direction (referred to as k in equation (3)) and one over the echoes measured in the v -direction (indicated by l), and is referred to as azimuth compression in SA terminology;

$$I(u_r, v_r, z_r) = \sum_k \sum_l I_{dat} \left(d_r^{k,l} \right) \cdot \exp \left(\frac{4\pi i}{\lambda} d_r^{k,l} \right) \quad (3)$$

where $I(\cdot, \cdot, \cdot)$ refers to the target response, I_{dat} to the value in the 3D raw data matrix and λ to the used wavelength. The result is shown in Fig. 3. The simulated point targets are represented by the crosses and the synthetic aperture result is shown by the iso-surfaces corresponding to a value of 10% beneath the maximum value of the target response in the 3D cube.

4. PERFORMANCE

4.1 Expected azimuth resolutions

In the synthetic aperture processing technique the azimuth resolution ρ is given by the size of the physical aperture size of the transmitting element D : $\rho = D/2$ [2]. Taking into

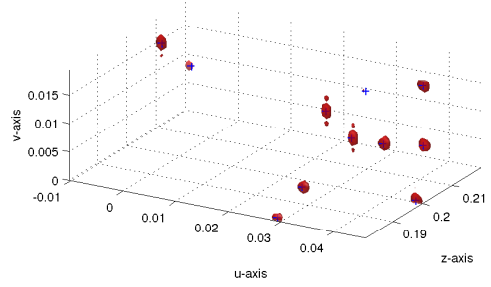


Figure 3: 3D synthetic aperture reconstruction. The crosses indicate the simulated target positions. The reconstruction is represented by the iso-surface taken at 10% beneath the maximum value of the target response in the 3D cube.

account that the opening angle is given by $\sin \theta_{u,v} \approx \lambda/D$, one can express the resolution ρ in u or in v as

$$\rho_{u,v} = \frac{c}{2f_0 \sin \theta_{u,v}}. \quad (4)$$

The expected resolution of THz images using the traditional imaging techniques is comparable to the one for very small opening angles. From Fig. 4 one can observe that for higher frequencies and broader opening angles the resolution improves significantly when applying SA processing. Comparing these theoretical resolutions with the ones obtained with traditional THz imaging (a resolution of 3 mm is obtained with a 0.2 THz CW system [8], resolutions of 2 to 3 mm are obtained using a pulsed system [4], [9]- [10]), indicates a possible improvement of at least a factor of 2. The figure also shows the obtained resolutions measured on the reconstruction results (indicated by the dots). How to derive those resolutions will be explained in detail in section 4.2.

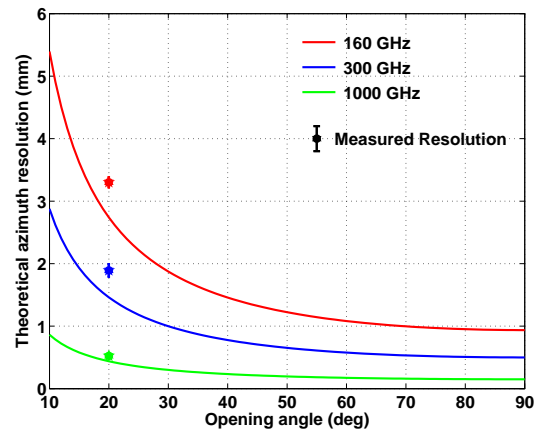


Figure 4: Theoretical azimuth resolution as function of beam opening for three carrier frequencies, i.e. 160 GHz, 300 GHz and 1 THz.

4.2 Obtained resolutions from the simulated data

In this paper 11 point targets have been simulated between $-0.01 \text{ m} \leq u_t \leq 0.05 \text{ m}$, $0 \text{ m} \leq v_t \leq 0.019 \text{ m}$ and $0.18 \text{ m} \leq z_t \leq 0.22 \text{ m}$. The synthetic aperture reconstruction is shown in Fig. 3 as explained in section 3. The resolutions are measured from these reconstruction results. The two parameters determining the obtained resolution (see section 4.1) are the carrier frequency f_0 and the opening angle θ of the transmitted beam. The opening angle in the u - (i.e. θ_u) and v -direction (i.e. θ_v) are considered to be equal in this analysis. To visualise the resolution dependency on the carrier frequency, 3 datasets were simulated for the respective carrier frequencies, $f_0 = 160 \text{ GHz}$, 300 GHz and 1 THz . To study the resolution dependency on the beam opening angle, 2 datasets were simulated once with a beam opening angle of $\theta = 20^\circ$ and once with a beam opening angle of $\theta = 30^\circ$. In Fig. 5 a representation of the synthetic aperture reconstruction is shown for one target, with a carrier frequency of $f_0 = 160 \text{ GHz}$, at a fixed depth corresponding to the depth location of one of the 11 simulated targets. The corresponding 3 dB resolutions in u and v are obtained by fitting a gaussian through the backscattered intensity along the u - and v -position of the target under study. The intensity on the y -axis is normalised to 1 in order to facilitate the comparison between the obtained resolutions. In the lower plot of Fig. 5 the improvement of the resolution as a function of increasing opening angle is clearly observed. One can also see that for a fixed opening angle and a fixed carrier frequency f_0 , the u and v resolutions are similar and that the obtained azimuth resolutions are very similar to the theoretical resolutions (see Fig. 4) for $f_0 = 160 \text{ GHz}$ (dots versus analytical curves). The mean resolution is taken over the u - and v -resolutions of the 11 targets and the error bar on the measured resolutions corresponds to the standard deviation.

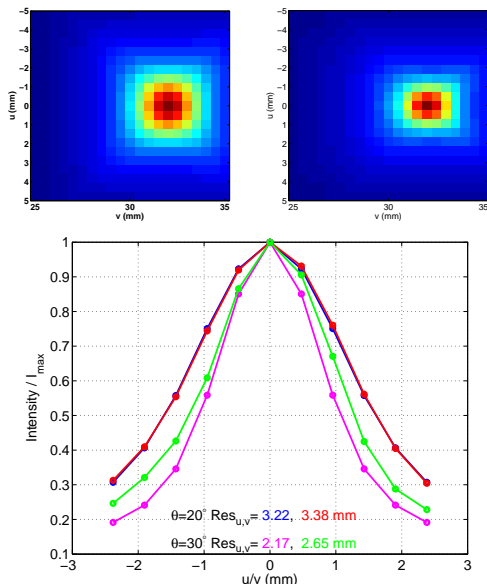


Figure 5: Target response resulting from the synthetic aperture reconstruction for $f_0 = 160 \text{ GHz}$ with an opening angle $\theta_{u,v} = 20^\circ$ (upper left) and $\theta_{u,v} = 30^\circ$ (upper right). Resolution dependency on opening angle for $f_0 = 160 \text{ GHz}$ (below).

In Fig. 6 the frequency dependency is shown for a fixed opening angle of $\theta_{u,v} = 20^\circ$. One clearly sees that the mean

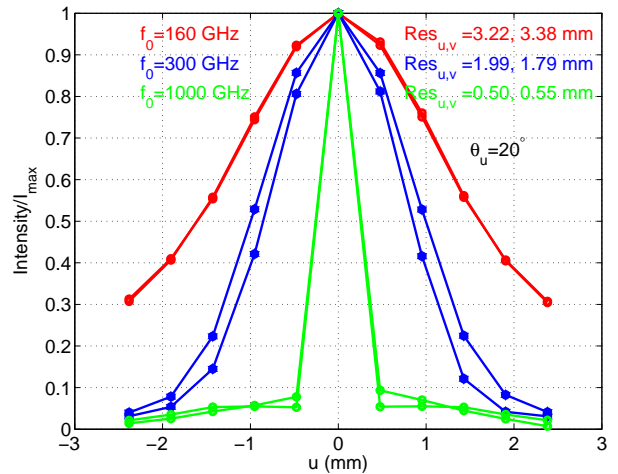


Figure 6: Azimuthal resolution dependency on frequency for u and v ($f_0 = 160, 300$ and 1000 GHz) and a fixed opening angle in u and v of 20° .

azimuth resolution over u and v improves from 3.3 mm for 160 GHz , to 1.9 mm for 300 GHz and 0.5 mm for 1 THz .

The depth (or range) resolution in z is only determined by the length of the transmitted pulse τ . For a τ of 1.2 ps a resolution is expected of $\alpha\tau c/2 \approx 0.3 \text{ mm}$ with $\alpha = 0.89$. The measured resolution in z (frequency independent) is equal to 0.53 mm .

4.3 Validity of the predicted SAT performance

Up till now predictions of the SAT performance have been formulated based on the synthetic aperture theory and simulated data. It is clear that this performance will be somewhat degraded when applying SAT on real data. These measurements are planned in the near future and an ISAT or Inverse SAT setup will be used: The THz system will be static and the testobject will move on a 2D-scanner. The validity of the predicted SAT performance, when extrapolating to real data, will depend on:

- **Source and detector coherence** A necessary condition to allow synthetic aperture processing is a phase stable source and detector. Otherwise the coherency between the data within the synthetic aperture length cannot be guaranteed.
- **Scanning precision** It is obvious that when the spatial position of the source and receiver with respect to the testobject is inaccurately determined during the data recording, an incorrect delay time will be measured. This will lead to an imprecise synthetic aperture summation and will consequently degrade the obtained resolution. Considering that the absolute spatial precision has to obey $\Delta d < \lambda/8$ [13], for a 1 THz wave (worst case) a spatial precision for the THz system position with respect to the testobject has to be less than 0.3 mm . Using a setup where the source and receiver device are fixed and where the testobject is placed on a moveable platform one should be able to fulfill this requirement in practice taking into account the specifications of existing scanning

systems.

- **Phase errors due to a varying propagation medium**
Another origin of phase errors can be due to the fact that the speed of light c with which the THz wave travels in vacuum slows down to a speed v_m for different materials. The lower speed depends on the material's relative permittivity ϵ_r , and its relative permeability μ_r as $v_m = c/n$ where $n = \sqrt{\epsilon_r \mu_r}$ indicates the refractive index.
- **Size of the opening angle and the signal to noise ratio**
Imaging with a high opening angle looks promising (see Fig. 5), however one has to consider that in the case of real data the dispersed signal due to the wide beam opening angle can fall below the noise level. The optimal opening angle will depend on the dissipated power of the source and the sensitivity of the detector used for the test measurements.

5. CONCLUSION

In this paper the synthetic aperture imaging technique has been applied in the THz domain and the two major benefits of this kind of processing versus the classical THz imaging have been demonstrated:

- The azimuth resolution in the two scanning directions u and v has been improved with respect to an imaging technique where no synthetic aperture is applied. For three different carrier frequencies (i.e. 160 GHz, 300 GHz and 1 THz) and two different opening angles (i.e. $\theta_{u,v} = 20^\circ$ and $\theta_{u,v} = 30^\circ$) corresponding resolutions have been derived from the synthetic aperture reconstruction result. A factor of about 2 to 3 is gained through the use of the synthetic aperture processing with respect to classical imaging techniques. All resolutions confirm the theoretically expected resolutions according to the synthetic aperture principles.
- The reconstruction algorithm is equally performant for all considered depths of the illuminated object.

These results promise a good applicability of the SA processing technique for NDT purposes. Future work will consist of creating a fast processing algorithm (which will operate in the frequency domain) before trying out the SA technique on data collected from real objects.

References

- [1] D. Abbott and X. C. Zhang. Scanning the issue: T-ray imaging, sensing and detection. In *Proceedings of the IEEE*, volume 95, pages 1509–1513, 2007.
- [2] I. G. Cumming and F. H. Wong. *Digital processing of synthetic aperture radar data*. Artech House, Boston, 2005.
- [3] K. P. Walsh, B. Schulkin, D. Gary, J.F. Federici, R. Barat, and D. Zimdars. Terahertz near-field interferometric and synthetic aperture imaging. In *Proc. SPIE*, Orlando, FL, USA, 2004.
- [4] J. O'Hara and D. Grischkowsky. Synthetic phased-array terahertz imaging. *Optics Letters*, 27(12):1070–1072, 2002.
- [5] K. McClatchey, M. T. Reiten, and R. A. Cheville. Time resolved synthetic aperture terahertz impulse imaging. *Applied physics letters*, 79(27):4485–4487, 2001.
- [6] R. Heremans, Y. Dupont, and M. Acheroy. Motion compensation on multiple receiver synthetic aperture sonar images. Vancouver, Canada, 2006.
- [7] M. Vandewal, R. Speck, and H. Suess. Efficient and precise processing for squinted spotlight sar through a modified stolt mapping. *EURASIP Journal on advances in signal processing*, 2007(59704), 2007.
- [8] A. Redo-Sanchez, N. Karpowicz, J. Xu, and X.C. Zhang. Damage and defect inspection with terahertz waves. *N. Darmouth, MA*, 2006.
- [9] R. F. Anastasi and E. I. Mandaras. Terahertz nde for metallic surface roughness evaluation. In *The 4th international workshop on ultrasonic and advanced methods for nondestructive testing and material characterization*, pages 57–62, 2006.
- [10] J. O'Hara and D. Grischkowsky. Quasi-optic terahertz imaging. *Optics Letters*, 26(23):1918–1920, 2001.
- [11] R. Heremans, M. Vandewal, and M. Acheroy. Synthetic aperture imaging extended towards thz sensors. In *7th IEEE Conference on sensors*, Lecce, Italy, 2008.
- [12] J. Kovaly. Synthetic aperture radar. *N. Darmouth, MA*, 1976.
- [13] P. Lacomme. *Air and Spaceborne Radar Systems, An introduction*. William Andrew Publishing, New York, 2001.